Progress In Electromagnetics Research B, Vol. 2, 115–124, 2008

SIMULATION OF ULTRA WIDEBAND MICROSTRIP ANTENNA USING EPML-TLM

M. Rajabi, M. Mohammadirad, and N. Komjani

Antenna and Microwave Research Laboratory
Iran University of Science and Technology
Iran

Abstract—In this paper the simulation of ultra wideband microstrip antenna is considered. Because of the ultra wideband characteristics of this antenna, it is better to use time domain simulation methods. In this work we use three dimensional transmission line matrix method (3D-TLM) and EPML-TLM algorithm for modeling PML boundary condition directly applied to TLM algorithm. Finally simulation results of some kinds of this antenna (e.g., linear tapered slot antenna and modified planar inverted cone antenna) are presented and compared with measurements and some commercial software's output.

1. INTRODUCTION

Transmission line matrix method (TLM) is one of the most efficient methods for calculation of electromagnetic fields [1, 2]. This method is based on the theory of transmission line and suitable for analyzing complex geometric structures. Furthermore in this method the frequency domain response over a wide bandwidth can be obtained with a single time domain simulation. Low dispersion, updating all the field components at the same time and same location and compatibility with the Berenger's separation technique, are main advantages of this method [3].

In this paper perfectly matched layer (PML) for simulation of free space is used. PMLs are layers initially designed by Berenger to simulate free space at the boundaries of FDTD computational domain [3]. The first attempt to implement PML algorithm to TLM method led to propose an inter-connected network between TLM and FDTD [4, 5]. Soon after, a uniform type of a 2D-TLM mesh for modeling usual and PML media was introduced. Following this work a new model based on the SCN node was developed by Dubard for

implementation of the Berenger's PML in 3D TLM method [6]. Two other types of 3D PML-TLM nodes were developed by authors [7]. The Extended PML-TLM (EPML-TLM) algorithm used in this paper performs well in TLM simulations and shows acceptable stability like FDTD method and more important there is no limitation on choosing time step unlike the other presented algorithms. Finally the simulation results of some types of ultra wideband microstrip antenna are presented.

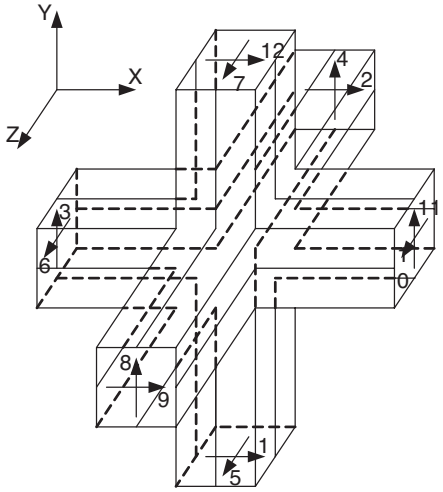

Figure 1. SCN node.

2. EPML-TLM ALGORITHM

A usual node in the TLM, shown in Fig. 1, for a homogeneous medium is SCN (Symmetric Condensed Node). The relation between incident and reflected voltages is determined by the scattering matrix S. The order of matrix S is 12×12 for homogeneous media and 18×18 for nonhomogeneous media. Electric and magnetic field components in each node are computed in term of the reflected voltages. To implement PML in the TLM by using SCN node according to the Berenger's technique, 6 field components are split into 12 components in the following form

$$\begin{aligned} E_i = & E_{ij} + E_{ik} \qquad H_i = H_{ij} + H_{ik}; \\ & (i,j,k) \in \{(x,y,z),(y,z,x),(z,x,y)\} \end{aligned} \tag{1}$$

The equation of electric field in a PML media is obtained as follows

$$\varepsilon_i\varepsilon_0\frac{\partial E_{ij}}{\partial t}+\sigma_{ej}E_{ij} = \frac{1}{\alpha_j}\frac{\partial H_j}{\partial j} \tag{2}$$

$$\varepsilon_i\varepsilon_0\frac{\partial E_{ik}}{\partial t}+\sigma_{ek}E_{ik} = \frac{1}{\alpha_k}\frac{\partial H_j}{\partial k} \tag{3}$$

where σ_{ei} is the electric conductivity along the oi, α_i is a coefficient greater than unity and ε_i is the relative permittivity of the media. Moreover, according to the matched condition in PML media [3] we have

$$\frac{\sigma_{ei}}{\varepsilon_i\varepsilon_0}=\frac{\sigma_{mi}}{\mu_i\mu_0} \tag{4}$$

Note that implementation of the algorithm depends on choosing suitable profiles for σ_{ei}, σ_{mi} and α_i. Some typical profiles are presented in [8], e.g., in the z direction

$$\begin{aligned}\alpha_z(z)&=1+\alpha_{\max}\left(\frac{z}{\delta}\right)^n\\ \sigma_{ez}(z)&=\sigma_{\max}\left(\frac{z}{\delta}\right)^n\end{aligned} \tag{5}$$

where n is the order of profile and $\alpha_{\max}$ and $\sigma_{\max}$ are determined as

$$\alpha_{\max} = (F_z-1)(n+1) \tag{6}$$

$$\sigma_{\max} = \frac{Ln\left|R_{prop}\right|}{-2Z_mS}\frac{(n+1)(2n+1)}{2n+1+\alpha_{\max}(n+1)} \tag{7}$$

Therefore to obtain the value of $\alpha_{\max}$ and $\sigma_{\max}$, it is necessary to estimate $|R_{prop}|$, F_z and n.

3. SIMULATION RESULTS

In this section the simulation results of the EPML-TLM algorithm for wideband microstrip antenna are presented and compared with those of HFSS, CST and also measurements.

3.1. Linear Tapered Slot Antenna (LTSA)

The structure of LTSA is shown in Fig. 2. Dielectric substrate is RT/Duriod 5880 with $\varepsilon_r = 2.2$ and $h = 0.78$ mm. The dimensions of this structure is listed in Table 1.

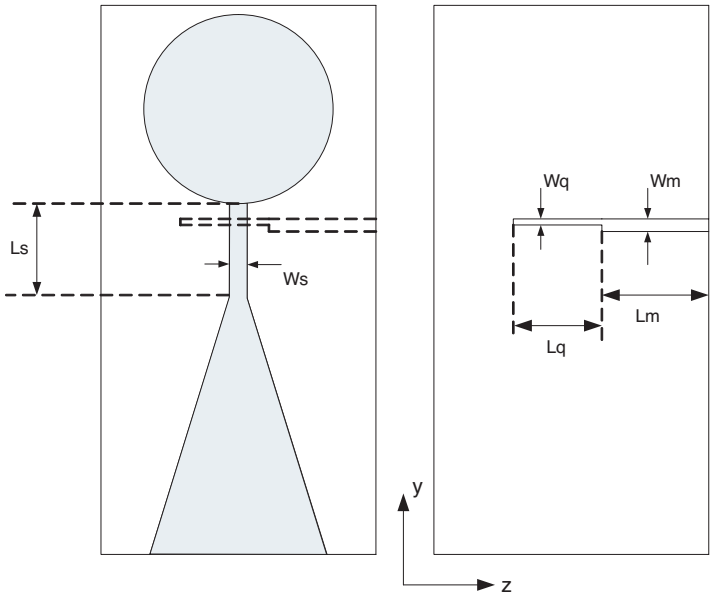

Figure 2. Structure of LTSA.

Table 1. Dimensions of the antenna shown in Fig. 2 in mm.

Substrate length	132	Substrate width	61
Ls	50	Ws	3
Lm	20	Wm	2.4
Lq	21.5	Wq	1.2
Cavity radius	20		

In simulation of this antenna the computational domain with $32 \times 262 \times 101$ cells is used where $\Delta x = 0.39\,\text{mm}$ and $\Delta y = \Delta z = 0.6\,\text{mm}$. Also the time step Δt is equal to 0.65 ps and number of PML cells used in x and y directions is 10 and 4 in z direction. For determining PML media we set $F_z = 3$, $n = 3$ and $|R_{prop}| = -100\,\text{dB}$. All of the PML cells are terminated by matched boundaries in each direction.

Considering antenna dimensions, the width of feed line, quarter wave transformer and slot line is modeled by 4, 2 and 5 nodes respectively. VSWR simulation result is plotted in Fig. 3 which is close to HFSS result. But there is a difference in small frequency range (near to 3 GHz) which can be referred to different conditions of simulations e.g., different number of cells for substrate width in two simulations.

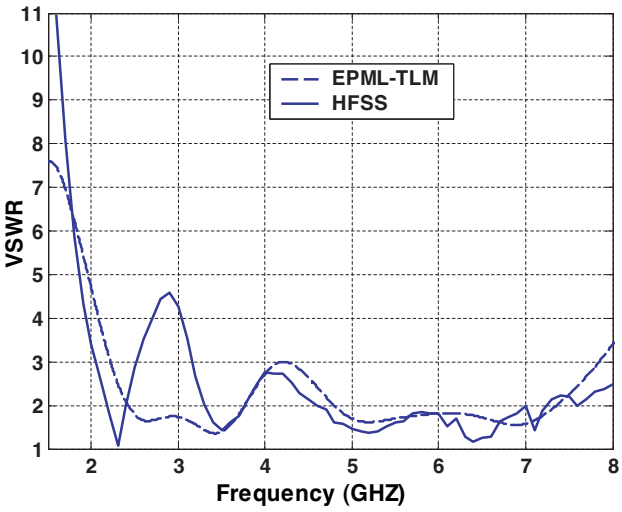

Figure 3. VSWR of simulated LTSA.

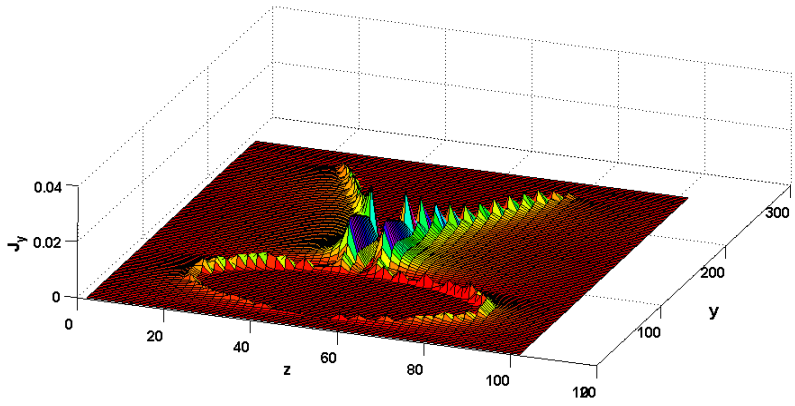

Figure 4. Amplitude of electric current in y direction.

The amplitude of electric and magnetic current on the surface of antenna is plotted in Fig. 4 and Fig. 5. These figures give better imagination about current behavior on the antenna surface and also show the effect of cavity and slot line. Note that the computation of electric and magnetic currents are done by using J_S and M_S equations

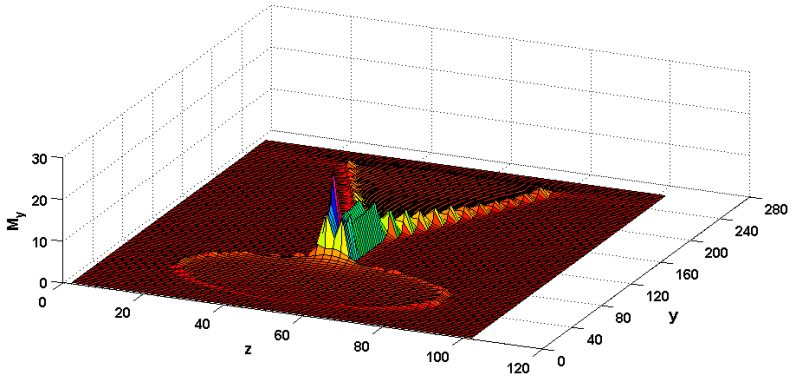

Figure 5. Amplitude of magnetic current in y direction.

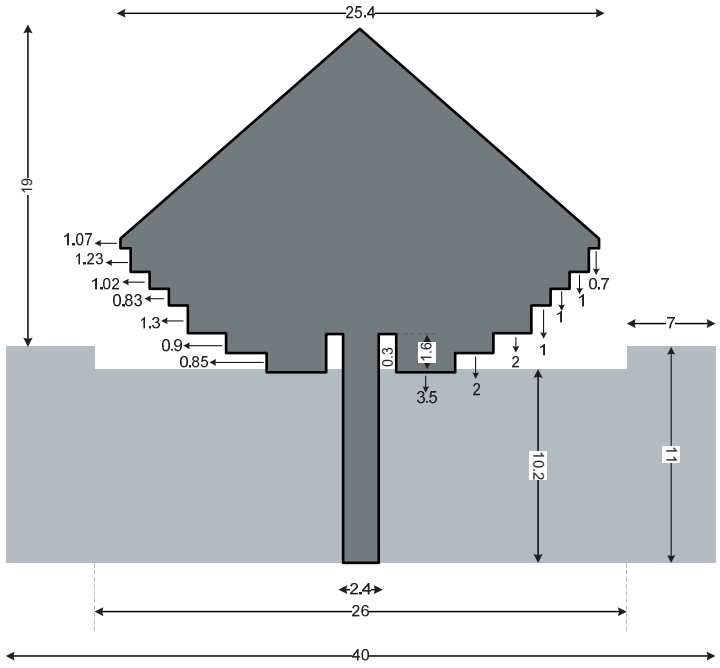

Figure 6. Modified PICA.

as follows

$$\vec{J_S} = n \times \vec{H} \tag{8}$$

$$\vec{M_S} = n \times \vec{E} \tag{9}$$

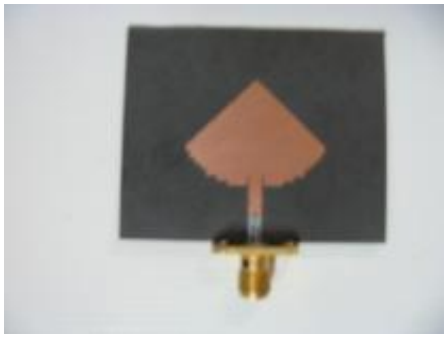

Figure 7. Fabricated antenna.

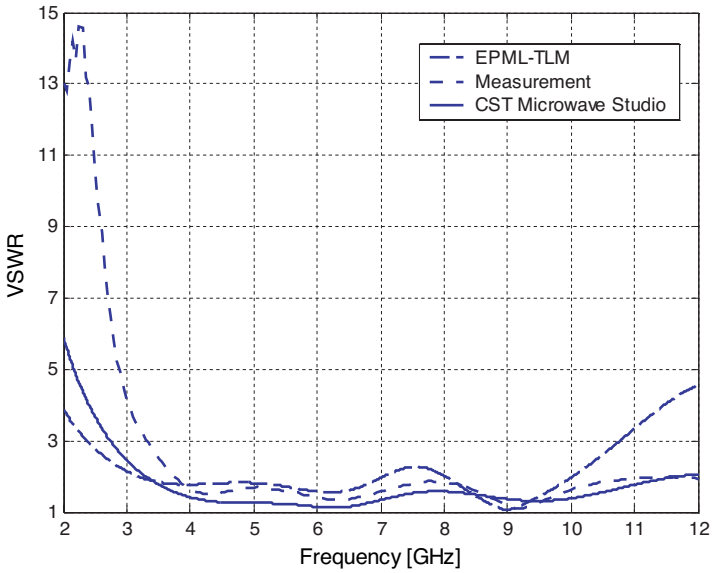

Figure 8. VSWR of MPICA without U-slot.

3.2. Modified Planar Inverted Cone Antenna (MPICA)

The purpose of this simulation is to design a planar monopole antenna with a step-shaped feed and compact size ($30 \times 40 \times 0.79\,\text{mm}^3$). This microstrip-fed antenna is a modified type of PICA (Planar Inverted Cone Antenna) [9] with additional modifications implemented in the

ground plane to increase impedance bandwidth [10, 11] by introducing two slits parallel to the feed line [11]. The geometry proposed for the antenna is shown in Fig. 6.

The step section shown in Fig. 6, resembles an arc with radius of 15 mm which causes an increase in bandwidth at lower frequencies of operation. Two slits used in parallel to microstrip line near the feed point also leads to further increase in bandwidth.

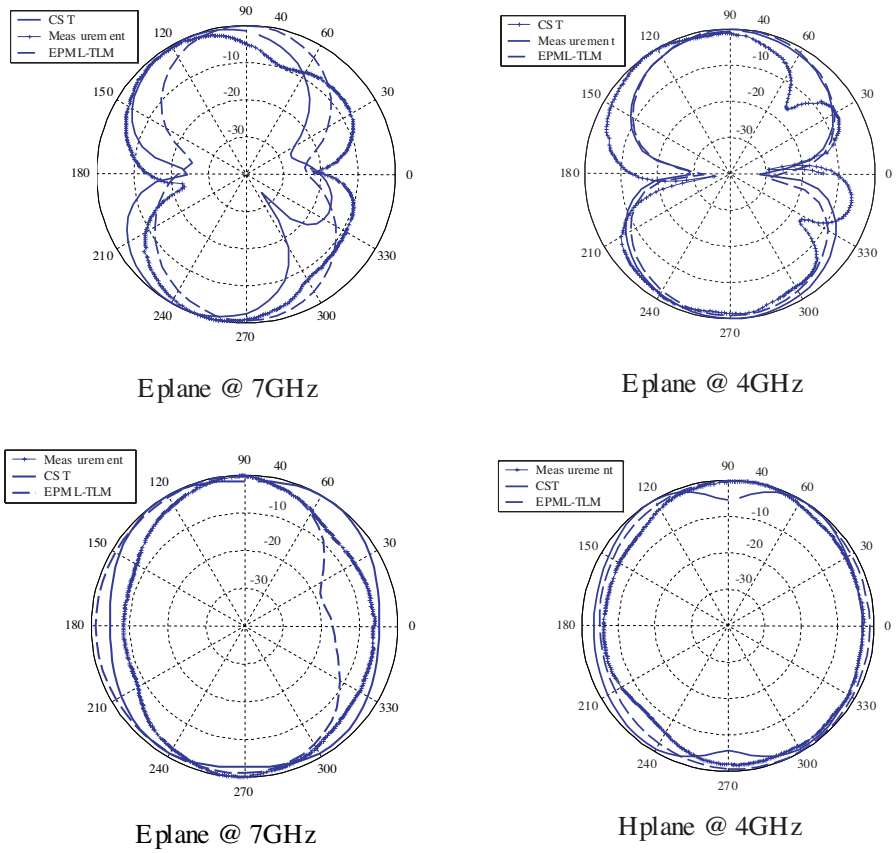

Figure 9. Radiation patterns of MPICA in E-plane and H-plane at 4,7 GHz.

In simulation of this antenna the computational domain with $165 \times 230 \times 74$ cells is used where $\Delta x = \Delta y = \Delta z = 0.2\,\text{mm}$. Also the time step Δt is equal to 0.33 ps and the number of PML cells in x, y and z directions is 5, 10 and 15 respectively. For determining PML media we set $F_z = 3$, $n = 3$ and $|R_{prop}| = -50\,\text{dB}$. All of the PML

cells are terminated by matched boundaries in each direction.

The fabricated antenna with dimensions $30 \times 40\,\text{mm}^2$ is printed on RT Duroid5870 ($\varepsilon_r = 2.33,\ h = 0.79\,\text{mm}$) substrate (Fig. 7) where length of the radiating element is about $\lambda_L/4$.

The measured and simulated VSWR of the antenna are shown in Fig. 8. Fig. 9 shows the simulated and measured radiation patterns at 4 and 7 GHz, in E-plane and H-plane. The proposed antenna has an almost omnidirectional pattern and there is good agreement in results of CST Microwave Studio, EPML-TLM and measurement.

4. CONCLUSION

In this work we showed the suitability of using EPML-TLM algorithm for wideband structures and complex geometries. For our purpose two different types of wideband microstrip antenna were chosen. The first structure is a slot antenna with a linear profile. The simulation results of this antenna were shown to be consistent with that of HFSS. The second structure is a modified type of PICA. VSWR in entire band and antenna patterns in E and H planes for two frequencies were derived as simulation outputs where we showed that the simulation results of EPML-TLM algorithm are in good accordance with CST software outputs and real measurements from fabricated antenna.

REFERENCES

1. Hoefer, W. J. R., "The transmission-line matrix (TLM) method," *Numerical Techniques for Microwave and Millimeter Wave Passive Structures*, T. Itoh (ed.), Wiley, New York, 1989.
2. Christopoulos, C., "The transmission-line modeling method: TLM," *IEEE/OUP on Electromagnetic Wave Theory*, IEEE Press, Piscataway, NJ, 1995.
3. Ney, M. M. and S. Le Maguer, "Diakoptics: An efficient technique for EMC applications," *Proc. Electromagnetic Compatibility*, 339–342, Zurich, Switzerland, 1999.
4. Eswarappa, C. and W. J. R. Hoefer, "Implementation of Berenger absorbing boundary conditions in TLM by interfacing FDTD perfectly matched layers," *Electron. Lett.*, Vol. 31, No. 15, 1264–1266, July 1995.
5. Pena, N. and M. M. Ney, "Absorbing-boundary conditions using perfectly matched layer (PML) technique for three-dimensional TLM simulations," *IEEE Trans. Microwave Theory Tech.*, Vol. 45, 1749–1755, Oct. 1997.

6. Dubard, J. L. and D. Pompei, "Optimization of the PML efficiency in 3-D TLM method," *IEEE Trans. on Microwave Theo. and Tech.*, Vol. 48, No. 7, July 2000.
7. Le Maguer, S., N. Pena, and M. M. Ney, "Matched absorbing medium techniques for full-wave TLM simulation of microwave and millimeter wave components," *Ann. Telecommun.*, Vol. 53, No. 3–4, 115–129, Mar.–Apr. 1998.
8. Le Maguer, S. and M. M. Ney, "Extended PML-TLM node: An efficient approach for full wave analysis of open structures," *Int. J. Numer. Model.*, Vol. 14, 129–144, 2001.
9. Suh, S.-Y., W. L. Stutzman, W. A. Davis, A. E. Waltho, K. W. Skeba, and J. L. Schiffer, "A UWB antenna with a stop-band notch in the 5-GHz WLAN band," *IEEE/ACES International Conference on Wireless Communications and Applied Computational Electromagnetics*, 2005.
10. Choi, J., K. Chung, and Y. Roh, "Parametric analysis of a band-rejection antenna for UWB application," *Microwave and Optical Technology Letters*, Vol. 47, No. 3, Nov. 2005.
11. Choi, W., J. Jung, K. Chung, and J. Choi, "Compact microstrip-fed antenna with band-stop characteristic for ultra-wideband applications," *Microwave and Optical Technology Letters*, Vol. 47, No. 1, Oct. 2005.
12. Lee, J., S. Park, and S. Lee, "Bow-tie wide-band monopole antenna with the novel impedance-matching technique," *Microwave and Optical Technology Letters*, Vol. 33, No. 6, June 2006.